SURFACE COMPOSITION OF THE BE LIMITERS AND THE STAINLESS-STEEL TORUS WALL AFTER OPERATION IN UNITOR

A.P. Martinelli, R. Behrisch,
H. Hammer[+], J. Hackmann[++]

IPP 9/60

December 1986

MAX-PLANCK-INSTITUT FÜR PLASMAPHYSIK

8046 GARCHING BEI MÜNCHEN

MAX-PLANCK-INSTITUT FÜR PLASMAPHYSIK

GARCHING BEI MÜNCHEN

SURFACE COMPOSITION OF THE BE LIMITERS AND THE STAINLESS-STEEL TORUS WALL AFTER OPERATION IN UNITOR

A.P. Martinelli, R. Behrisch,
H. Hammer[+], J. Hackmann[++]

IPP 9/60 December 1986

[+]Institut für Angewandte Physik, Universität Düsseldorf,
D-4000 Düsseldorf, FRG

[++]Physikalisches Institut II, Universität Düsseldorf,
D-4000 Düsseldorf, FRG

This report is an extended version of a paper with the same title presented at the Plasma-Surface Interaction Conference at Princeton, 5-9 May 1986, to appear in Journal of Nuclear Materials, 1987.

Die nachstehende Arbeit wurde im Rahmen des Vertrages zwischen dem Max-Planck-Institut für Plasmaphysik und der Europäischen Atomgemeinschaft über die Zusammenarbeit auf dem Gebiete der Plasmaphysik durchgeführt.

SURFACE COMPOSITION OF THE BE LIMITERS AND THE STAINLESS- STEEL TORUS WALL AFTER OPERATION IN U N I T O R

A.P. Martinelli[+], R. Behrisch[+], H. Hammer[++], J. Hackmann[+++]

[+]Max-Planck-Institut für Plasmaphysik, EURATOM Association, D-8046 Garching/München, FRG

[++]Institut für Angewandte Physik, Universität Düsseldorf, D-4000 Düsseldorf, FRG,

[+++]Physikalisches Institut II, Universität Düsseldorf, D-4000 Düsseldorf, FRG

Abstract

The surfaces of two Be limiters and of a test sample from the stainless-steel torus wall used in UNITOR were analyzed by RBS, PIXE, AES, and SEM/EIXE. The main foreign atoms found on the limiters are O (2 x 10^{17} to 2 x $10^{18}/cm^2$), Fe, Ni, Cr and Sn (2 x 10^{15} to 2 x $10^{16}/cm^2$). There are no large differences in the foreign atom coverage on the different surface areas of the limiters. Generally, the front surfaces of the limiters show slightly lower coverage than the sides. On limiter 2, the Sn coverage is about a factor of 4 larger than on limiter 1, indicating that the Sn source was close to this limiter. The stainless-steel test sample from the torus wall shows islands of BeO, which can be attributed to splashes or droplets eroded from the limiters during disruptions. Major erosion of the limiters occurred only during the first 100 shots, when many discharges were terminated by disruptions. Redeposited wall material is found on the wall sample which partly covers the BeO deposits. The surface modifications of limiters and wall samples were discussed by taking into account the particle fluxes from and to the walls and limiters.

TABLE OF CONTENTS

1. Introduction

The use of graphite as a low-Z material for the construction of limiters in large tokamaks has led to a reduction of metal impurities and an improvement of the plasma parameters. This improvement was found in spite of the observation that the carbon limiters as well as carbon wall samples taken from different tokamaks (ASDEX, TFTR, TFR, JET) had become coated during plasma operation with metal deposits corresponding to up to 100 monolayers /1-4/. Another interesting candidate as low-Z material for limiters is beryllium, which has been used up to now only in two tokamaks /5,6,7/. One major reason for this limited use is its toxic properties. In UNITOR the use of Be limiters had revealed improved performance of the discharge and reduction of the metallic impurity level by a factor of approximately ten. In addition, beryllium showed a further advantage, because it is an effective getter for oxygen. Oxygen is a major impurity in most tokamaks and sputtering by oxygen ions can be the dominant process for metal atom release from the vessel walls. In this work, several surface and surface layer analysis techniques were used to determine the composition of the Be limiters used in the UNITOR tokamak and of a test sample from the stainless-steel (304) torus wall. The wall modifications are discussed by considering the particle fluxes from and to the walls and limiters. These fluxes have previously been measured /8/.

2. Experimental

The UNITOR vacuum vessel with the arrangement of the two poloidal Be limiters and the position of the wall sample is shown in fig. 1a. UNITOR can be operated either with a toroidal limiter or with one or more poloidal limiters. In the first case the poloidal limiters are retracted behind the torus wall, which serves as toroidal limiter (see fig. 1b, left). By moving the Be tiles radially into the torus (up to 30 mm) UNITOR can be operated in the poloidal limiter mode (see fig. 1b, right). The Be limiters were used at various radial positions for about 1200 discharges, each having a plasma current I_p = 50 kA, a magnetic field B_T = 1.7 T, and a plasma density $n_e = 2 \times 10^{13}/cm^3$ giving

plasma temperatures of kT_e = 200 eV and kT_i = 50 eV at discharge times of 50 ms. This operation results in a total exposure time of the Be limiters to the plasma of approximately 60 s. The energy deposition on the limiters is of the order of 100 J/cm^2 per discharge with a peak power load of 2 kW/cm^2, while the corresponding numbers for the wall load are about one order of magnitude lower. During a normal discharge the power density on the limiters was about 0.7 kW/cm^2. The temperature increase of the Be limiters measured immediately following a discharge was a few kelvin. The temperature increase of the Be limiter surface during a discharge was estimated (thermoshock calculation) to be a few tens of kelvin.

During the test period the limiters were exposed to a variety of different operational conditions in order to investigate the compatibility of Be with the tokamak plasma and its influence on impurity production. The test series was performed in three steps:

1) After insertion of the Be limiters the torus was pumped down and the pulsed cleaning discharge was operated for two days. This procedure is normally applied in UNITOR after ventilation of the torus and provides a clean machine ready for proper tokamak operation. In this case, however, only poor performance of the machine was achieved, as indicated by a high amount of disruptive shots (40 %). This behaviour drastically changed after a few major disruptions causing severe melting and erosion on limiter No. 2 for a length of about 40 mm, and a width of about 1 mm, along the edge towards the electron drift side (see fig. 1a). After this, only very few discharges (3 %) were disruptive for the entire test period. There was no further heavy erosion on either limiter.

2) During the second phase UNITOR was operated while the radial positions of the poloidal limiters were changed. The content of Cr, O, and Be in the plasma was investigated spectroscopically. A reduction of the concentration of metallic impurities by a factor of ten was found. The results are reported in detail in /6/.

3) The third experimental phase started with a long period (15 days) of intense cleaning of the torus without tokamak operation, while the poloidal limiters were retracted to the same position as the toroidal limiter. The torus was then ventilated with air and pumped down, after which the reduction of the oxygen content in the plasma was monitored after intermittent cleaning of the vessel. This procedure was applied in order to check the ability of the cleaning method on a beryllized torus. No remarkable change compared with prior observations without beryllium could be observed. Finally, the cleaning discharge was operated for 1 hour in methane to investigate the formation of beryllium carbides. In this state of the torus and limiter surfaces no proper tokamak action could be achieved. So the carbon was removed by cleaning in hydrogen. After a few tokamak shots the test was terminated and the two Be limiters and the wall test sample were removed from the torus before chemical decontamination of the torus started. It should be noted that the pulsed cleaning discharge was always active (e.g. overnight) except when the machine was switched for tokamak operation.

The shape and dimensions of the limiters and the samples cut off for surface analysis are shown in fig. 2a. The analysis was performed along the dashed lines as indicated. From the two side strips (60 x 5 x 2.5 mm^3) the surface of sample D had been oriented toward the electron drift side, while the surface of sample E had been oriented toward the ion drift side. The surfaces of the three front strips A,B,C (27 x 8 x 1.5 mm^3) were exposed to the plasma nearly parallel to the magnetic field direction. The geometry of the stainless-steel wall sample (10 x 240 mm^2) is given in fig. 2b, the longer side being cut in the poloidal direction. The shaded areas were studied by AES and EIXE.

3. Surface analysis techniques

The following analysis techniques were used.

1) Rutherford Backscattering Spectroscopy (RBS) was done with ^4He ions of 2 MeV at a backscattering angle of 165^o; analyzed depth about 400 nm. The RBS technique is especially applicable for the detection of higher-Z elements on a lower-Z substrate.

2) Particle Induced X-ray Emission (PIXE) analysis was performed with 1.5 MeV protons. The actual depth analyzed is given by the escape depth of the X-rays. Owing to the Be/BeO window in front of the X-ray detector only elements with $Z \geq 20$ could be detected. Quantitative results are obtained by calibration with known surface films. All results are given in atoms/cm^2, which may be distributed within the surface layer analyzed. The actual depth analyzed is about 8 µm.

3) Auger Electron Spectroscopy (AES) provides information on the composition and chemical binding in a shallow surface layer of about 1 nm. Depth profiling was carried out by Ar^+ sputtering. The results are only semi-quantitative.

4) Scanning Electron Microscopy (SEM) and Electron Induced X-ray Emission (EIXE) were performed with 30 keV (10 keV) electrons and a Si(Li) detector. SEM was used to analyze the surface topography, while EIXE provides results similar to those of PIXE with information on the global chemical composition down to a depth of about 1 to 5 µm. Low-Z elements, such as Be, C, O, are not detected, because, as in the PIXE measurements, the Si(Li) detector is protected by a Be(BeO) window, which absorbs the low-energy X-ray lines. The lateral resolution of the SEM is typically $\leq$ 100 nm, the data presented being given in relative numbers.

4. Results

4.1 Analysis of the Be limiters

A first survey of the surface composition of the limiters was made by AES. Figure 3 shows the main elements found on limiter sample 1B by measuring stepwise across a shallow sputter crater which was produced shortly before the measurement inside the spectrometer. The crater has a diameter of 7 mm and a depth of 10-20 nm. Each point in fig. 3 corresponds to a different depth, the crater bottom being at position 5. We see a uniform depth profile of Be and O (upper diagram), which indicates a thick BeO layer at the limiter surface.

Furthermore, N and C do not depend on the depth and appear in the spectra in a chemically bound form. Stainless-steel components (in fig. 3, bottom, represented by Fe) and also Sn, Ca, S are present as a surface coverage of nonuniform thickness which was partly sputtered away during crater formation. The average number of atoms within the surface layers of the Be limiters was measured by RBS and PIXE. Examples of ^{4}He RBS spectra for an unexposed target and a plasma-exposed part of the limiter are shown in fig. 4. The unexposed Be was obtained by machining away a 0.05 mm thick layer from the plasma-exposed sample of target 2D.

In the RBS spectrum of the unexposed Be (fig. 4a) an average oxygen coverage of about 3×10^{16} atoms/cm^2 is found, which corresponds to a coverage of about 10 to 20 monolayers of BeO. In addition, a small concentration of heavy impurities is found in the Be, the masses of each of these being identified in the PIXE spectrum. The RBS spectrum of the exposed target (fig. 4b) shows considerably more oxygen corresponding to a one to two orders of magnitude larger coverage than in the unexposed target. Further peaks corresponding to a surface deposition of C, of Ti, Cr, Fe, Ni and of Sn are found.

The PIXE spectra measured at the same points as the RBS spectra are shown in figs. 5a and 5b. In the unexposed target the elements S, Cl, Sn, Ca, Cr, Fe, Ni, Cu, Au are found. At the plasma-exposed sample

nearly the same elements are seen, but some of them in much larger quantity. The Fe concentration measured by PIXE for the unexposed Be target was about 3.4×10^{16} atoms/cm^2. Assuming an X-ray emerging depth of 5 to 10 μm, this gives a Fe volumetric concentration of 10^{-3} to 5×10^{-2} in the Be. This Fe concentration was always subtracted from the measured values of the Fe concentration on the Be limiter.

The average distributions of foreign atoms measured on limiters 1 and 2 are shown in figs. 6a and 6b, respectively.

- The amount of deposited oxygen was determined from the RBS spectra only. Because the oxygen peak is not well separated from the C peak and the Be edge, it was evaluated by means of two different background subtraction schemes corresponding to a minimum and a maximum oxygen coverage. This gave values of 2×10^{17} to 2×10^{18} O atoms/cm^2.
- For Fe, a major component of stainless steel, the PIXE measurements gave a deposition of 1.1×10^{16} Fe atoms/cm^2 after background subtraction. This compares reasonably well with the value of 0.7×10^{16} Fe, Ni, Cr atoms/cm^2 obtained by RBS.
- Furthermore, the Be limiters were found to be covered with Sn atoms, which were clearly identified in the PIXE spectrum. The total amount is about 10 monolayers on limiter 2, and a factor of 4 lower on limiter 1.
- Besides these main impurities, a deposition of S, Cl, Ca, Cu and Au was found, but could not be evaluated quantitatively.

Generally, all foreign atoms are very uniformly distributed over the entire limiter surface. The differences are mostly within the measuring uncertainty. Only on limiter 1 is the Fe coverage on side 1E (ion drift side) nearly one order of magnitude larger than on side 1D (electron drift side). Furthermore, the front surface shows a slightly lower impurity coverage than the sides. Figure 6c shows the spatial distributions of Fe, Sn and O on Be limiter No. 2 along the analysis trace 2B on the front face of the limiter; and the same on the side faces of the limiter (central points of analysis traces 2E and 2D in fig. 2a).

Figure 7 gives an example of an EIXE spectrum taken from a selected point on sample 1B. The spectrum corroborates the elemental composition of the limiter surface found by the other methods. Some of the foreign elements are mainly present as contamination in the bulk material (e.g. Al, Si, S, Cl, Cn, Zn), others cover the surface, mainly atoms from the stainless- steel torus wall. It should be noted that the EIXE spectra show large spatial variations both in species and in intensity. Finally, fig. 8 shows a SEM picture from sample 2D (electron drift side), where the main erosion occurred during a disruption in the early phase of the test series. One sees macroscopic cracking and melting and it is likely that a large amount of beryllium was eroded and distributed inside the torus during this event.

4.2 Analysis of the stainless-steel wall sample

At the beginning of the analysis it was necessary to sputter away a carbon film stemming from the carbonization test during the final experimental phase. After that the spatial distribution of Be/BeO and impurities on the stainless-steel substrate were analyzed by AES. The result of sample No. 6 is given in fig. 9. This distribution displays a nonuniform island structure of Be/BeO deposited on the torus wall. Beryllium is always accompanied by increasing oxygen deposition. Uniform coverage of the wall by Be and/or BeO was not found, although it cannot be excluded that there might be a very thin cover of BeO. Furthermore, the AES spectra show that the same foreign elements are present on the wall surface as are found on the Be limiters. The analysis of the other wall samples marked in fig. 2 showed no remarkable differences from sample 6.

EIXE spectra from two selected spots of wall sample No. 6 are shown in fig. 10. One of the spectra has a characteristic structure (e.g. in the low energy range) compared with a spectrum taken from a nearby spot on the stainless-steel substrate. This spectrum is very similar to those taken from Be samples and shows the same foreign elements also present in unexposed beryllium. At the place where the spectrum was taken the SEM picture shows a droplet-shaped object with a dimen-

sion of about 50 µm (see fig. 11). It is possible that this is a piece of molten limiter material eroded during a disruption. The presence of Cr, Fe and Ni lines in the EIXE spectrum indicates coverage by stainless-steel components deposited during later discharges. Additionally, SEM pictures show some droplets and splashes containing mainly stainless-steel components. An example is shown in fig. 12.

5. Discussion

The various analysis methods applied to the beryllium limiters and the wall sample all show a large number of different foreign elements present at the surfaces. According to their sources we can identify three groups of foreign elements:

1. Elements which are present as impurities in the bulk material of the beryllium limiters, namely S, Cl, Sn, Ca, Cr, Fe, Ni, Cu, Au.
2. Elements which were present in UNITOR before and which stem from earlier limiter tests (Al_2O_3, TiC, graphite, SiC). The sources for the Sn coverage on the limiters and the K and Na deposits could not be identified. Tin might come from previous tests: also, the possibility of Sn segregating from the Be bulk upon melting (disruption, limiter 2) is not excluded.
3. In the following discussion we focus on the main surface impurities Fe, Cr, Ni and O deposited on the Be limiters and on the Be deposited on the wall sample. Since the particle fluxes from and to the walls and limiters are quite well known in UNITOR (see /8/), we can compare the sputter yields and the deposits on the surfaces.

5.1 Surface modification of the Be limiters

5.1.1 Surface coverage by foreign atoms

PIXE and RBS analyses gave a coverage of 1×10^{16} Fe atoms/cm^2 on the Be limiter surface. The coverage with Fe is slightly larger on the ion drift side than on the electron drift side and the front surface. When the toroidal stainless-steel limiter was used, the release of metallic impurities in UNITOR /8/ was measured to be 1×10^{17} Fe atoms per discharge. The majority of metal impurities are thought to be sputtered

by oxygen, carbon, and also by the metals themselves. The observed reduction of metallic impurities by a factor of ten when Be limiters are used supports the conclusion that only 1 x 10^{16} metal atoms per discharge are released from the stainless-steel wall, i.e. a total amount of 1.2 x 10^{19} metal atoms are released from the stainless-steel wall after 1200 discharges. If we further assume that 50 % of these impurities is scraped away by the Be limiters the coverage should be approximately 1.5 x 10^{17} Fe atoms/cm^2 on the limiters and 3 x 10^{14} Fe atoms/cm^2 redeposited on the first wall. This is one order of magnitude larger than found on the limiter surfaces. The explanation for this discrepancy could be re-erosion of deposited material from the limiter surface.

Oxygen is detected by RBS with a depth resolution of 10-20 nm to 10^{17} - 10^{18} atoms/cm^2. From AES spectra it can be deduced that oxygen is mainly present in the form of BeO down to a depth of about 20 nm. The oxygen flux onto the limiters has been estimated at approximately 1.4 x 10^{15} cm^{-2} per discharge. This means a total load after 1200 discharges of 1.7 x 10^{18} O atoms/cm^2. This value fits the observations quite well. An interesting point is that RBS and AES analysis reveal BeO down to a depth of about 50 monolayers. As oxygen should not diffuse so far into the bulk, it is presumed that at elevated temperatures Be migrates to the surface. There are also indications that BeO has a lower sputter yield than Be itself. This could be a favourable effect with respect to the long-time gettering properties of Be.

5.1.2 Surface topology

SEM pictures show molten areas mainly at the electron drift side of the Be limiter, but also on the front side. At temperatures close to the melting point there will probably be enhanced erosion and ejection of Be/BeO droplets. Similar effects were observed in the ISX-B experiment /6/. The molten areas show also large cracks and holes due to thermal stresses (see fig. 8).

5.2 Surface modification of the stainless-steel wall

5.2.1 Surface coverage by foreign atoms

The ablation of molten material from the beryllium limiters was observed in UNITOR only during the first discharges terminated by disruptions. During normal discharges the main release process is sputtering of Be by incident protons. The flux of protons in UNITOR onto the limiters is 6×10^{20} protons/s (50 % of the total flux; energy ~ 50 eV). This results in a sputter yield of approximately 3×10^{17} Be atoms per discharge. After 1200 discharges we should have a Be deposit on the torus wall of 2.3×10^{16} Be atoms/cm^2, assuming uniform redeposition. On the wall sample investigated the AES spectra do not show this quite high uniform Be coverage. The spectra show isolated BeO spots of various sizes clearly situated on top of the surface and covered by a thin film of stainless-steel components. The thickness of this film was estimated to be approximately 10^{14} atoms/cm^2, as mentioned above.

We conclude that during disruptions some droplets and clusters of molten limiter material travel in the toroidal direction and are redeposited on the torus wall. In this experiment the wall sample under investigation was 45° in the toroidal direction away from the nearest Be limiter. Furthermore, most of the released limiter material is redeposited directly in the vicinity of the limiters. Swap and scratch samples taken from various parts of the torus wall immediately after opening of the machine reveal a two order of magnitude higher Be coverage close to the limiters than at the location of the wall sample.

5.2.2 Surface topology

On the wall surface we see droplets and splashes of molten wall material. Only few traces of arcing are found on the wall sample. Furthermore, we find some ball-shaped objects which are most probably Be/BeO because their EIXE spectra show a similar composition to spectra from blank Be samples (S, Cl, C, Ca). The size of these objects typically varies between 1 and 50 µm.

6. Summary

The results of the surface analysis of the beryllium limiters and the torus wall by RBS, PIXE, AES and EIXE revealed some important details for understanding the efficacy of Be in reducing metallic impurities in UNITOR:

1. There is no uniform coverage of the torus wall by Be to protect the wall material from being sputtered. To a greater extent, the reduction of metallic impurities is caused by effective gettering of oxygen, which in UNITOR has been identified as producing the largest sputter yield of wall material /8/.

2. Beryllium is mainly present in the form of BeO. At the limiters surfaces, there is a rather thick layer ($\geq$ 50 monolayers) of BeO. This result supports the assumption that at higher temperatures Be migrates from the bulk material to the surface, where it getters oxygen. Furthermore, BeO seems to be sputtered less than Be.

3. Enhanced erosion of the limiters is observed when the temperature of the Be limiters is raised to near the melting point. In UNITOR this only happens during disruptions. In this case, droplets and clusters of molten limiter material are released from the limiter and can be found on the torus wall even at large distances from the limiters.

4. In the case of UNITOR, as in other tokamaks, the limiters are contaminated by large amounts of wall material.
   Even the beryllium deposits found on the torus wall are covered by stainless-steel components. This fact implies that for an efficient reduction of metallic impurities in the plasma the first wall surface should consist of the same material as the limiters. All areas of the first wall show erosion and redeposition. Depending on the details of the first-wall geometry, there are some areas where erosion is greater than deposition, as on limiters. In areas more remote from the plasma, deposition predominates over erosion. In

principle, only the erosion-dominated areas should consist of the same material as the limiters. All areas finally also become covered by this material. This equilibrium state is attained faster, however, if the deposition-dominated areas are also initially covered with a thin layer of limiter material.

5. Even though the limiters were exposed to the cleaning discharge for long periods of time, we have no evidence that this had any effect on the surface modification. As the energy of the cleaning discharge is low ($kT_e \sim 1$ eV), there might be only minor effects on loosely bound wall and limiter deposits.

7. Acknowledgement

We should like to thank B.M.U. Scherzer, Garching, for helping with the accelerator analysis and E. Englert, Garching, for his advice in the use of the computer programs for data evaluation, and H. Schmidl, Garching, for assistance during the measurements.

8. References

/1/ Behrisch, R., P. Børgesen, J. Ehrenberg, B.M.U. Scherzer, B.D. Sawicka, J.A. Sawicki and the ASDEX Team
J. Nucl. Mat. 128 & 129 (1984), 470

/2/ Doyle, B.L., W.R. Wampler, H.F. Dylla, D.K. Owens, M.L. Ulrickson
J. Nucl. Mat. 128 & 129 (1984), 955

/3/ TFR Group (presented by A. Grosman)
J. Nucl. Mat. 128 & 129 (1984), 292

/4/ Ehrenberg, J., R. Behrisch, A.P. Martinelli, H. Kukral
IPP - JET Report No. 29, May 1985

/5/ Edmonds, P.H., K.J. Dietz, P.K. Mioduszewski, R.D. Watson, L.C. Emerson, W.A. Gabbard, D. Goodall, J.E. Simpkins, J.L. Yarber, J. Vac. Sci. Technol. A3 (1985), 1100

/6/ Isler, R.C., K. Behringer, E. Källne, P.D. Morgan, N.J. Peacock, P.H. Edmonds, P.K. Mioduszewski, E.A. Lazarus, P.L. Lomas, C.H. Ma, M. Murakami, R.V. Neidigh
Nucl. Fusion 25 (1985), 1635

/7/ Hackmann, J., J. Uhlenbusch
J. Nucl. Mat. 128 & 129 (1984), 418

/8/ Reinhold, G., J. Hackmann, J. Uhlenbusch
J. Nucl. Mat. 121 (1984), 231

Figure Captions

Fig. 1a: Top view of UNITOR and the arrangement of limiters and wall sample.

Fig. 1b: Cross-section of UNITOR:
left: toroidal limiter configuration,
right: poloidal limiter configuration.

Fig. 2a: Be limiter and location of the samples cut off for surface analysis.

Fig. 2b: Stainless-steel wall sample. The shaded sections were used for AES and EIXE analyses.

Fig. 3: AES analysis of Be sample 1B:
The data were measured across a crater formed by sputtering shortly before the measurements. The values therefore display a depth profile.

Fig. 4: RBS analysis of Be target 2D:
The upper spectrum was taken for comparison from an unexposed target obtained by machining away a 0.05 mm thick layer.

Fig. 5: PIXE analysis of the same part of the Be limiter shown in fig. 4.

Fig. 6: Summary of RBS and PIXE results for the main contaminants found on the Be limiters (O, Fe, Sn):
a) limiter No. 1,
b) limiter No. 2,
c) spatial distribution on the central part of limiter No. 2.

Fig. 7: EIXE spectra of two small spots on Be limiter 1B displaying the large number and local variation of foreign elements present at the limiter surface.

Fig. 8: SEM picture of limiter sample 2D (electron drift side).

Fig. 9: Local variation of foreign atoms on the stainless-steel wall sample No. 6. The figure shows the spotwise deposition of BeO on the torus wall.

Fig. 10: EIXE spectrum of a beryllium droplet (identified by the characteristic co-elements Na, Si, S, K) on wall sample No. 6. For comparison, a spectrum of a point in the vicinity showing only stainless-steel components is plotted, too.

Fig. 11: A SEM picture of the area where the spectrum of fig. 10 was taken shows a spherical object with a diameter of about 50 µm.

Fig. 12: Stainless-steel splash on the wall sample. Many of these splashes and droplets are found on the samples.

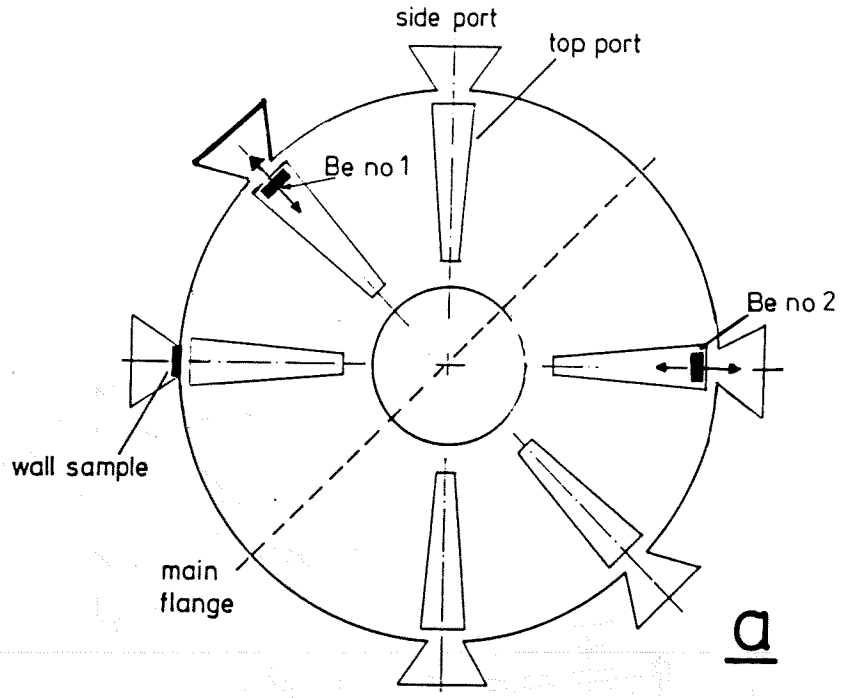

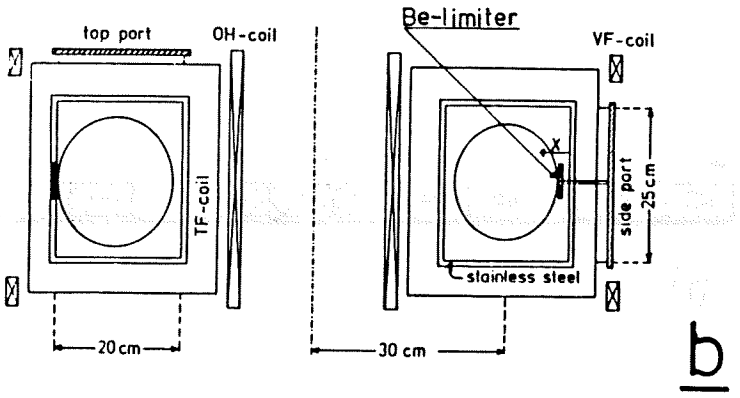

Fig. 1a: Top view of UNITOR and the arrangement of limiters and wall sample.

Fig. 1b: Cross-section of UNITOR:
left: toroidal limiter configuration,
right: poloidal limiter configuration.

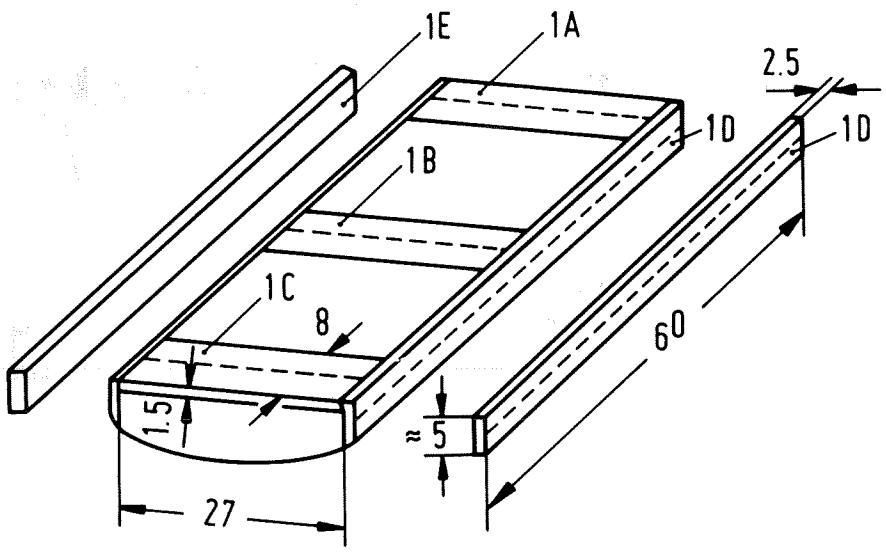

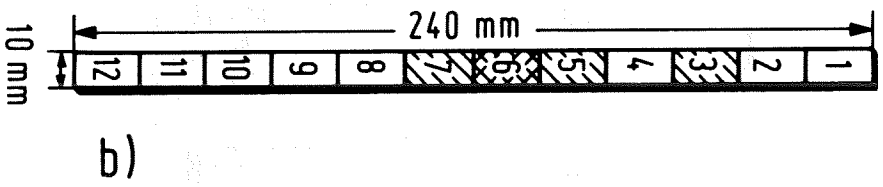

Fig. 2a: Be limiter and location of the samples cut off for surface analysis.

Fig. 2b: Stainless-steel wall sample. The shaded sections were used for AES and EIXE analyses.

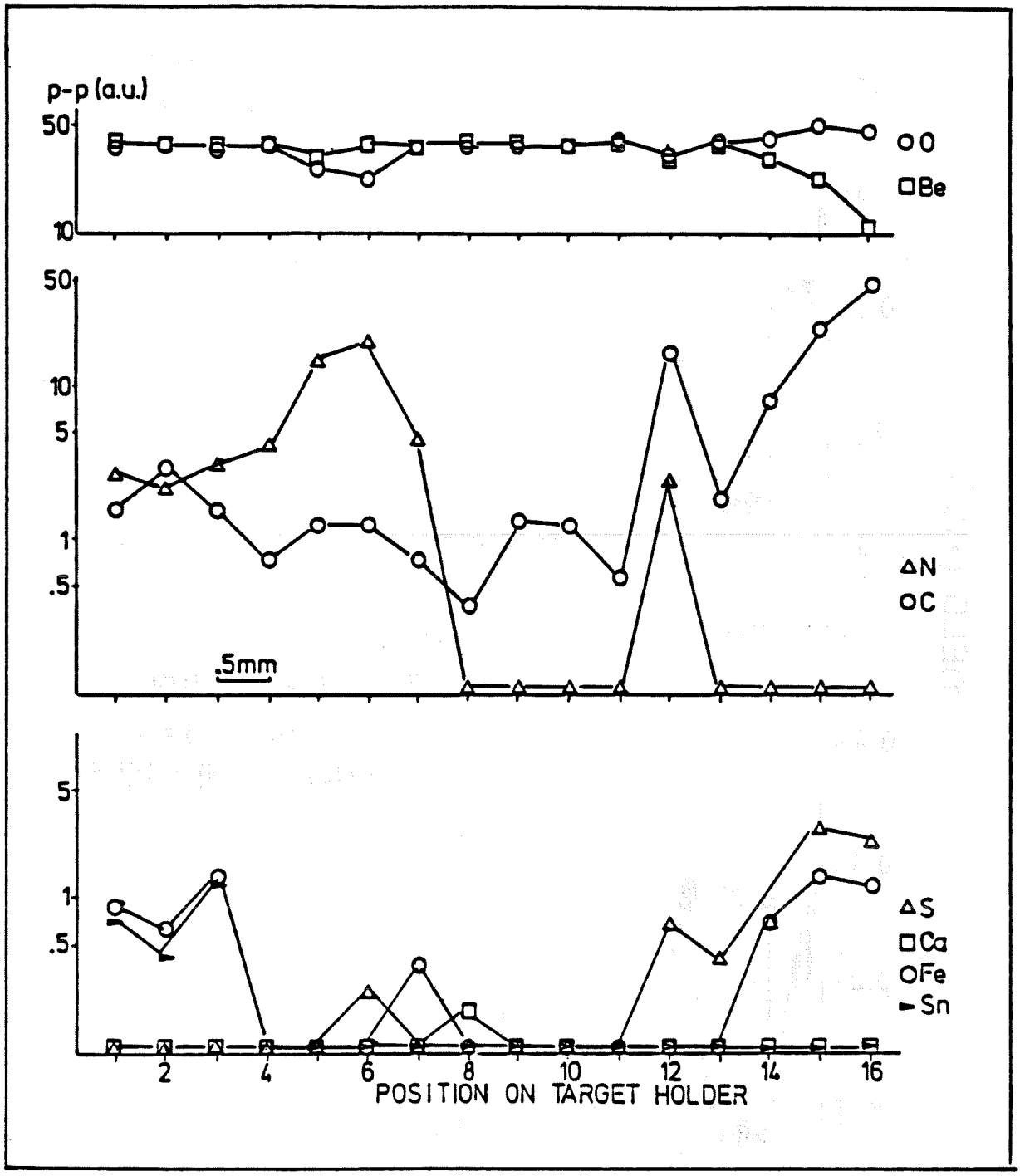

Fig. 3: AES analysis of Be sample 1B:
The data were measured across a crater formed by sputtering shortly before the measurements. The values therefore display a depth profile.

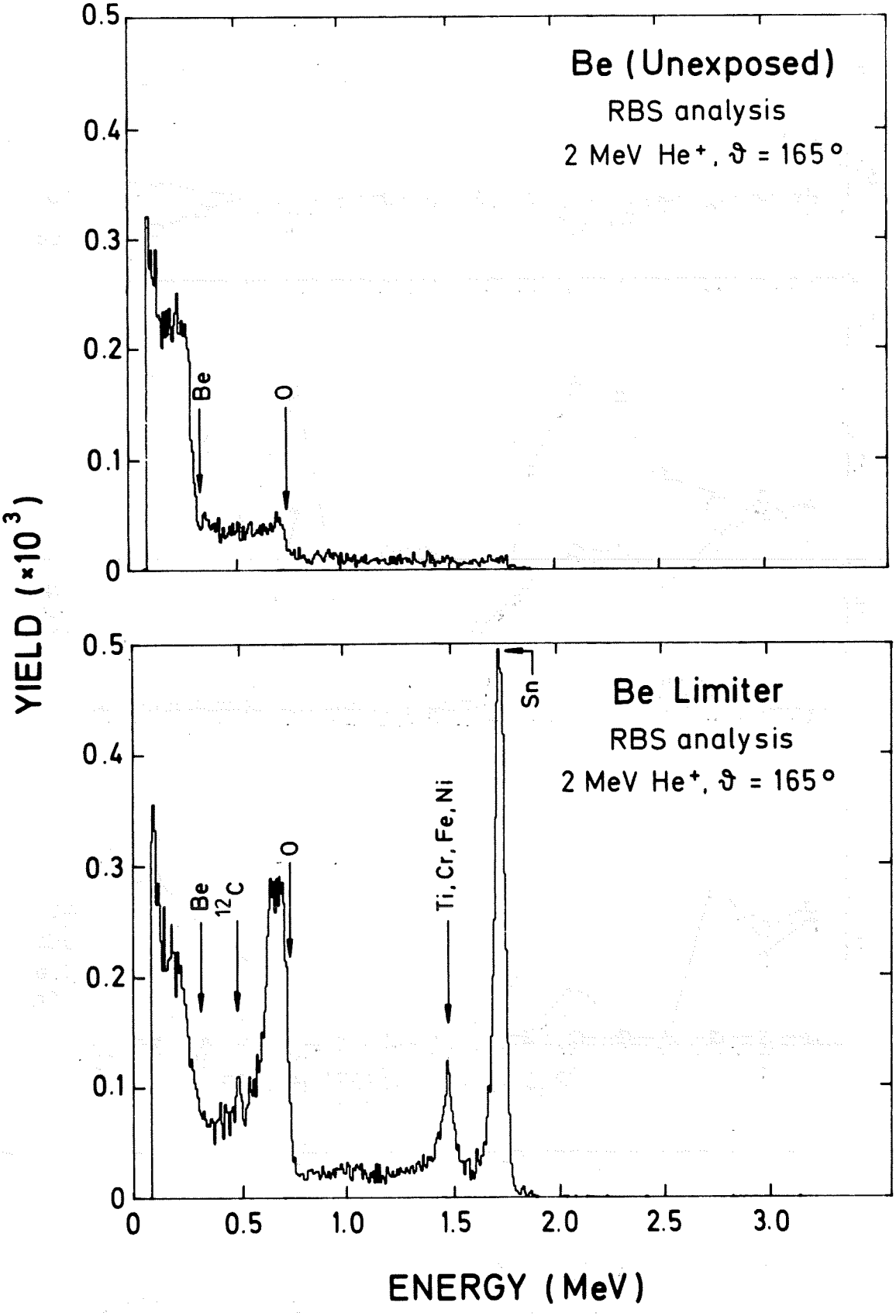

Fig. 4: RBS analysis of Be target 2D:
The upper spectrum was taken for comparison from an unexposed target obtained by machining away a 0.05 mm thick layer.

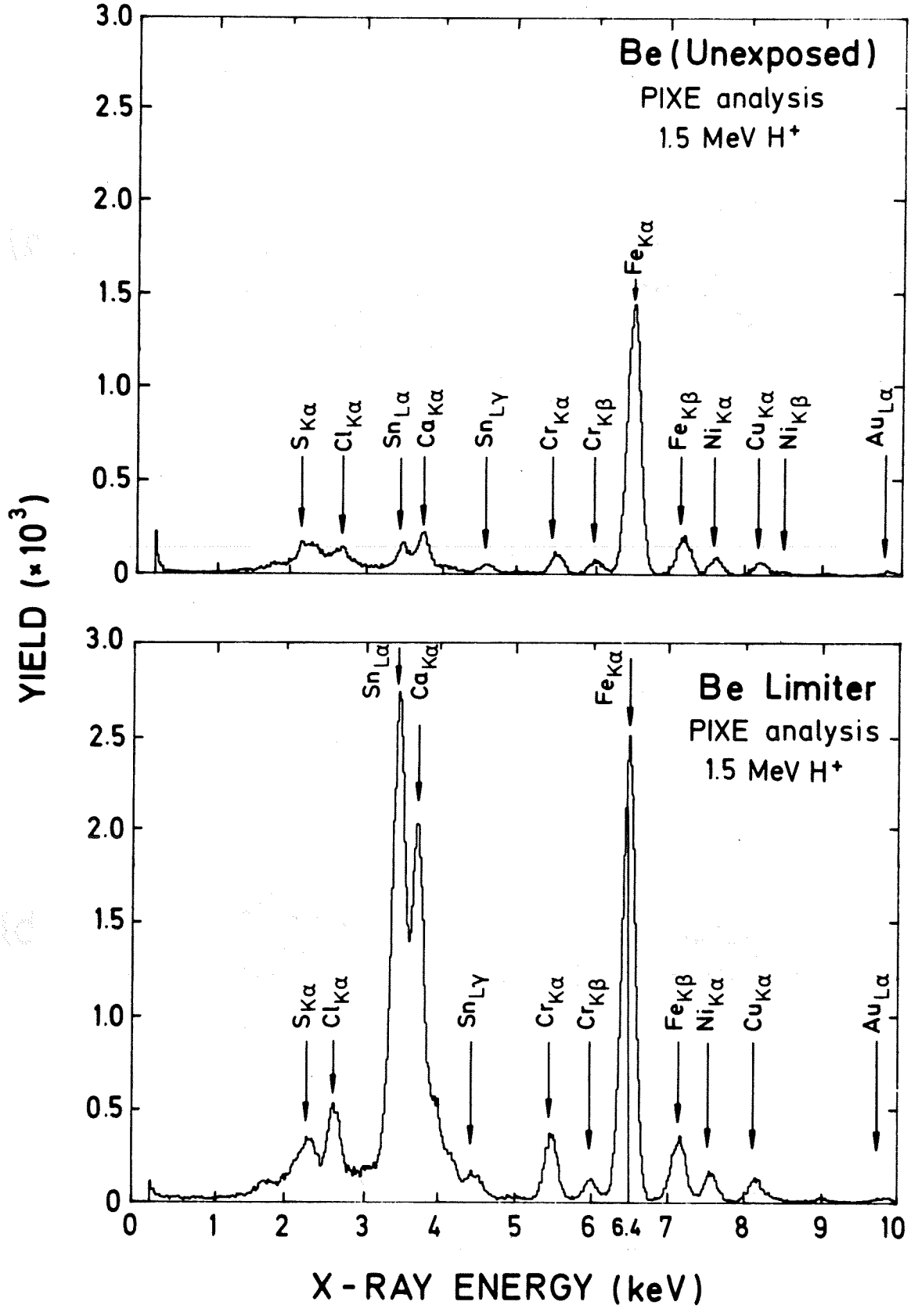

Fig. 5: PIXE analysis of the same part of the Be limiter shown in fig. 4.

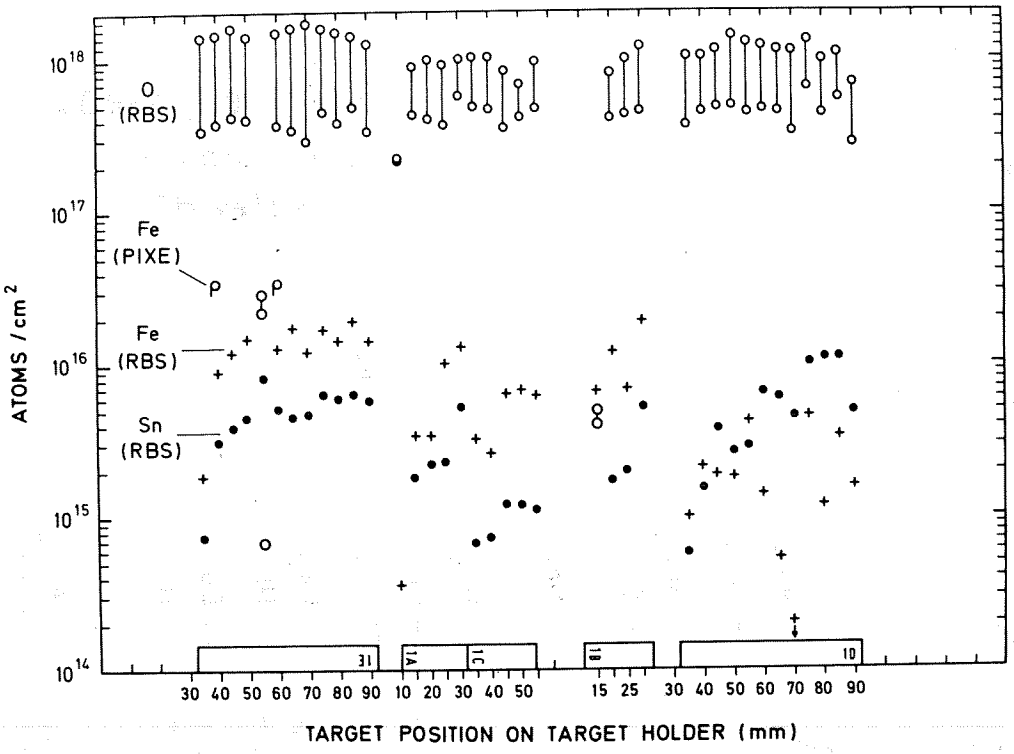

a)

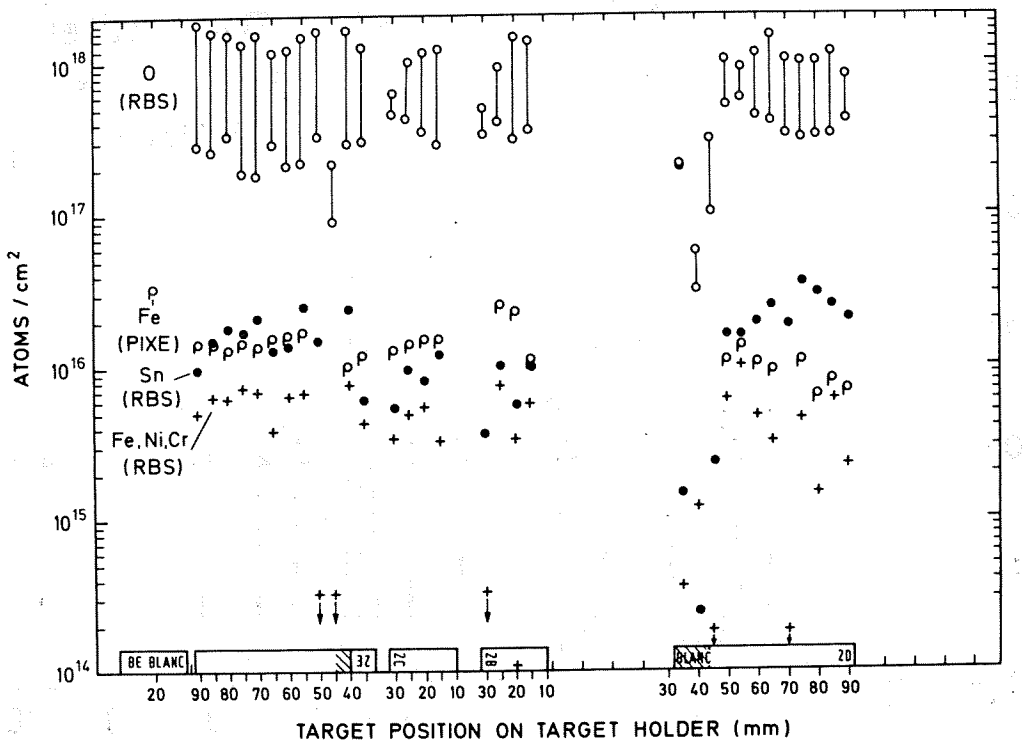

b)

Fig. 6: Summary of RBS and PIXE results for the main contaminants found on the Be limiters (O, Fe, Sn):
a) limiter No. 1,
b) limiter No. 2.

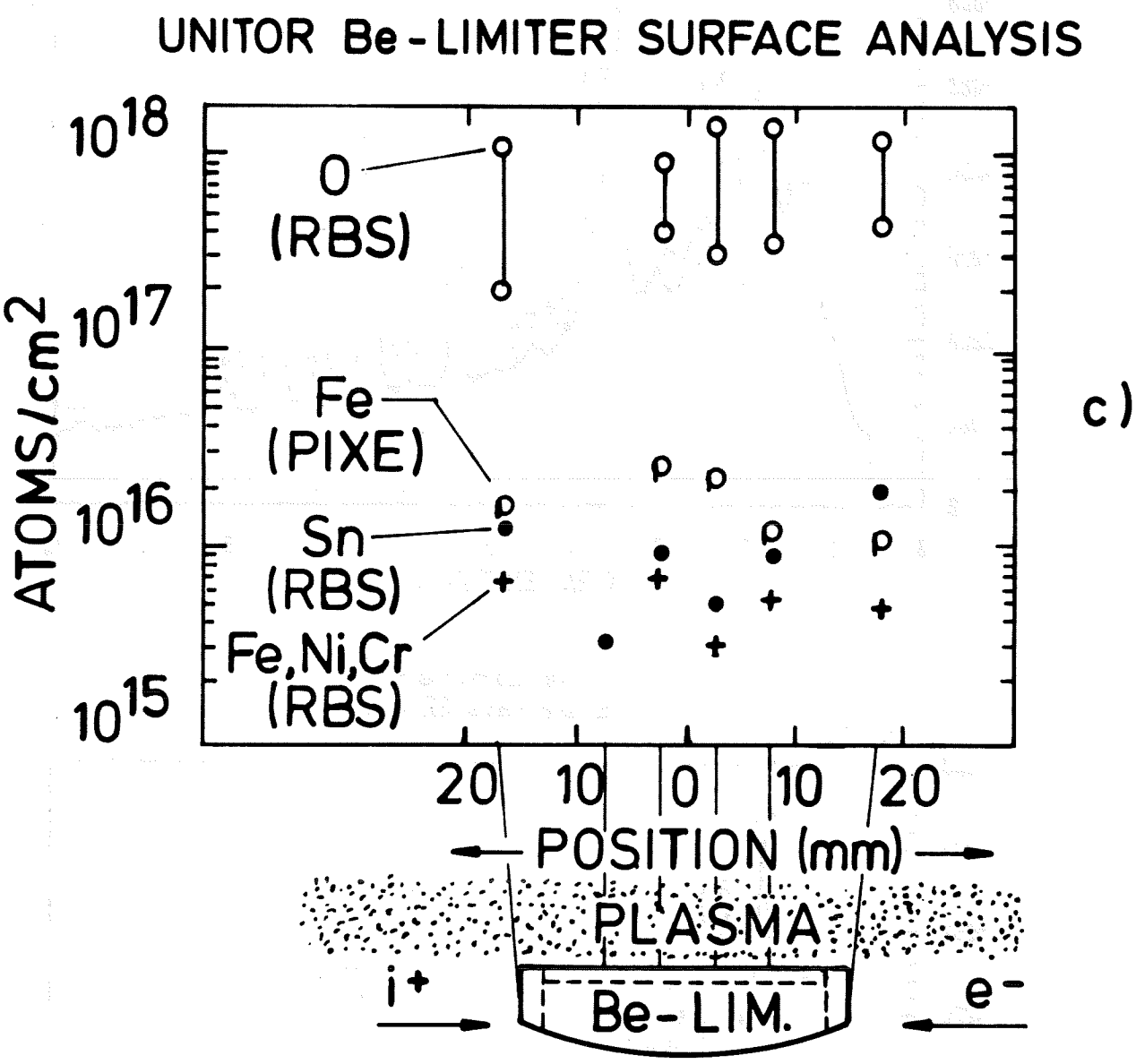

Fig. 6: Summary of RBS and PIXE results for the main contaminants found on the Be limiters (O, Fe, Sn):

c) spatial distribution on the central part of limiter No. 2.

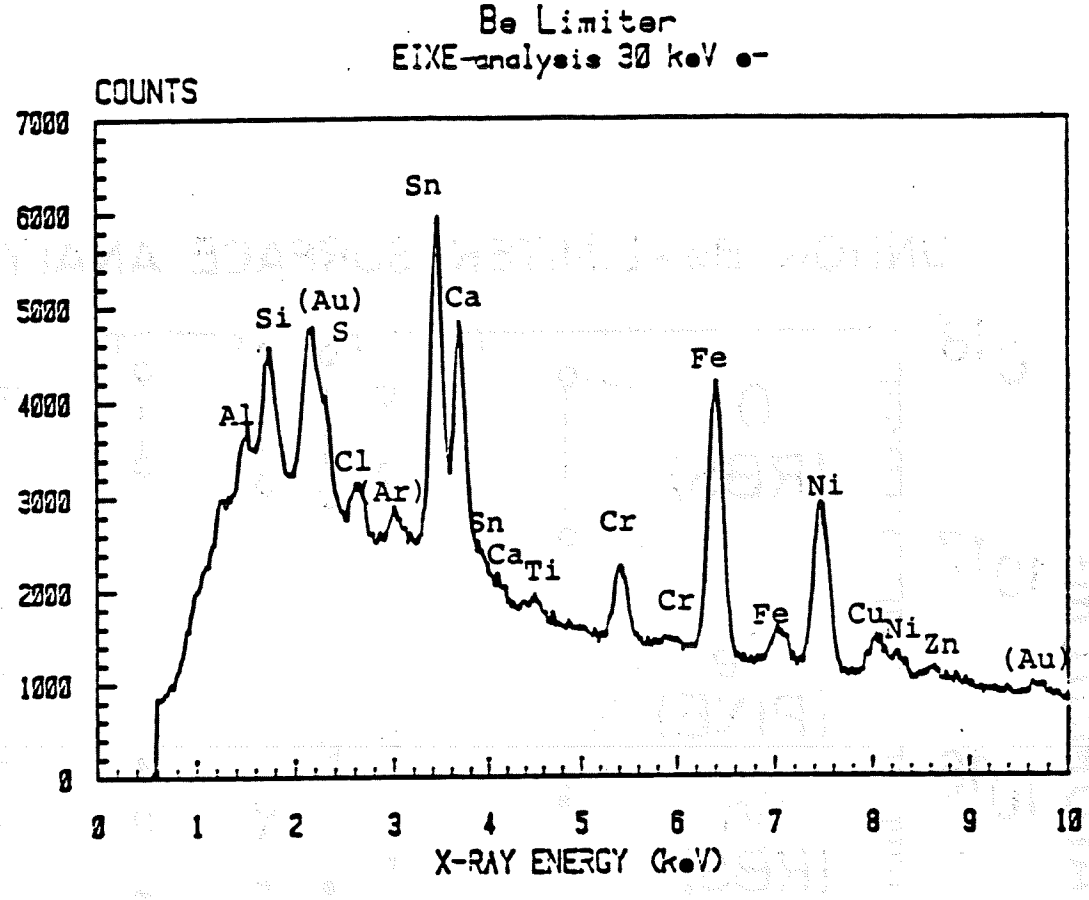

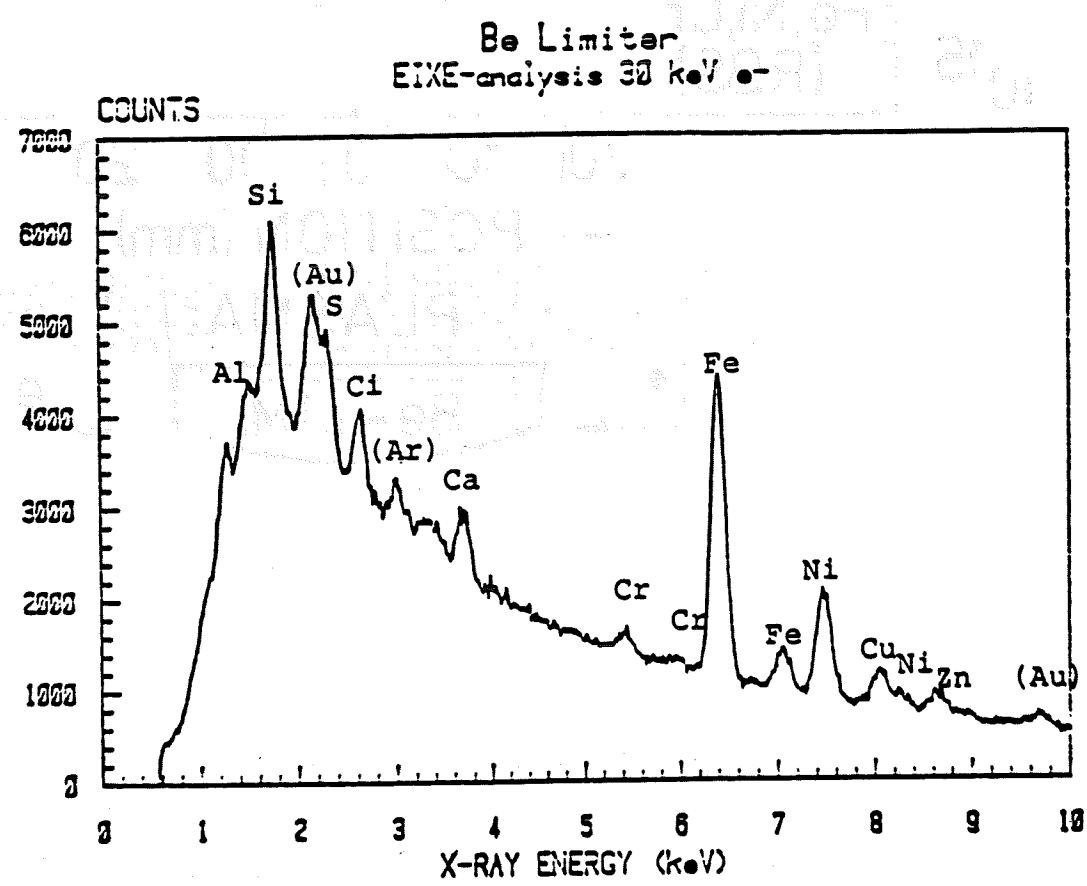

Fig. 7: EIXE spectra of two small spots on Be limiter 1B displaying the large number and local variation of foreign elements present at the limiter surface.

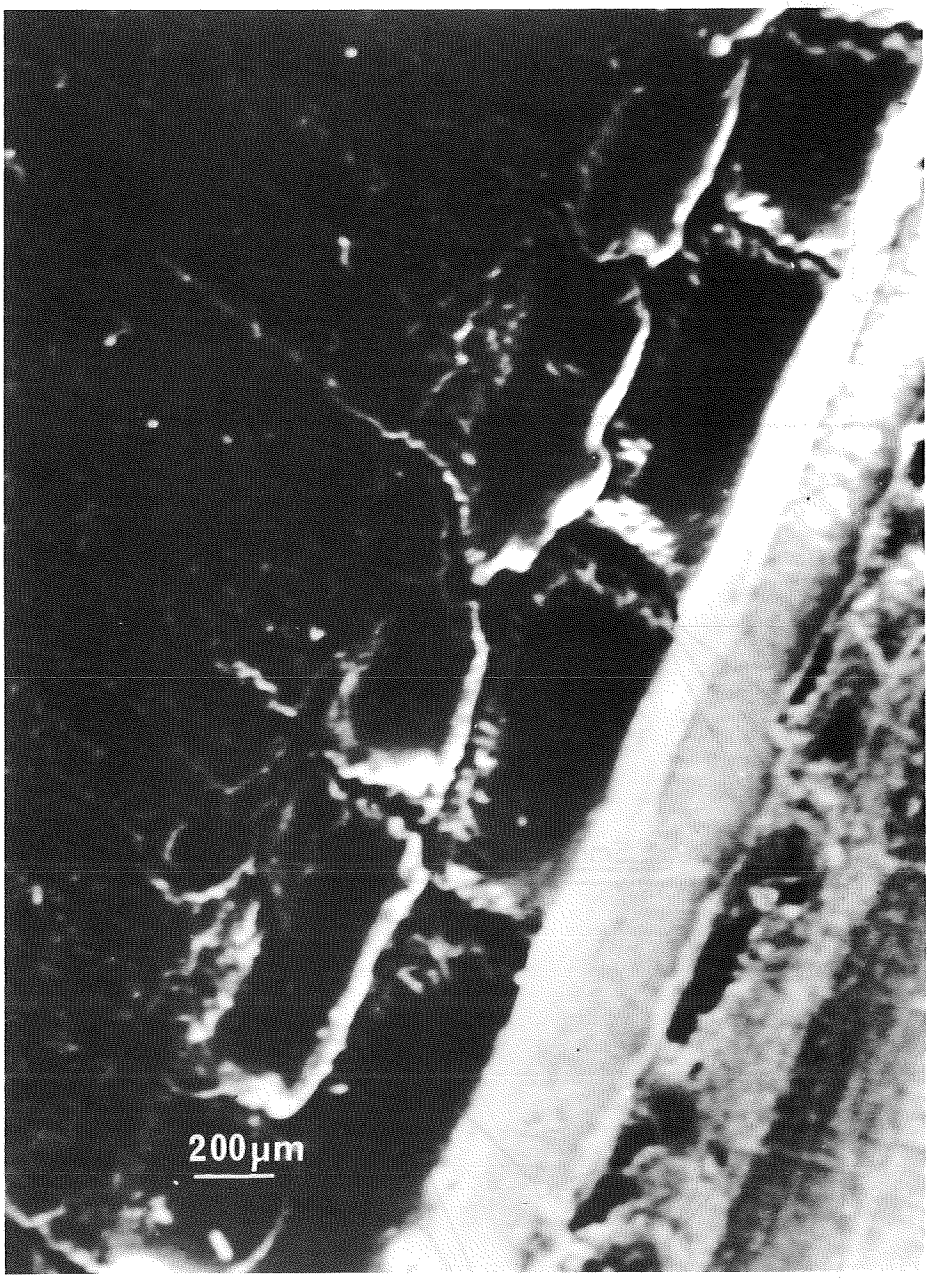

Fig. 8: SEM picture of limiter sample 2D (electron drift side).

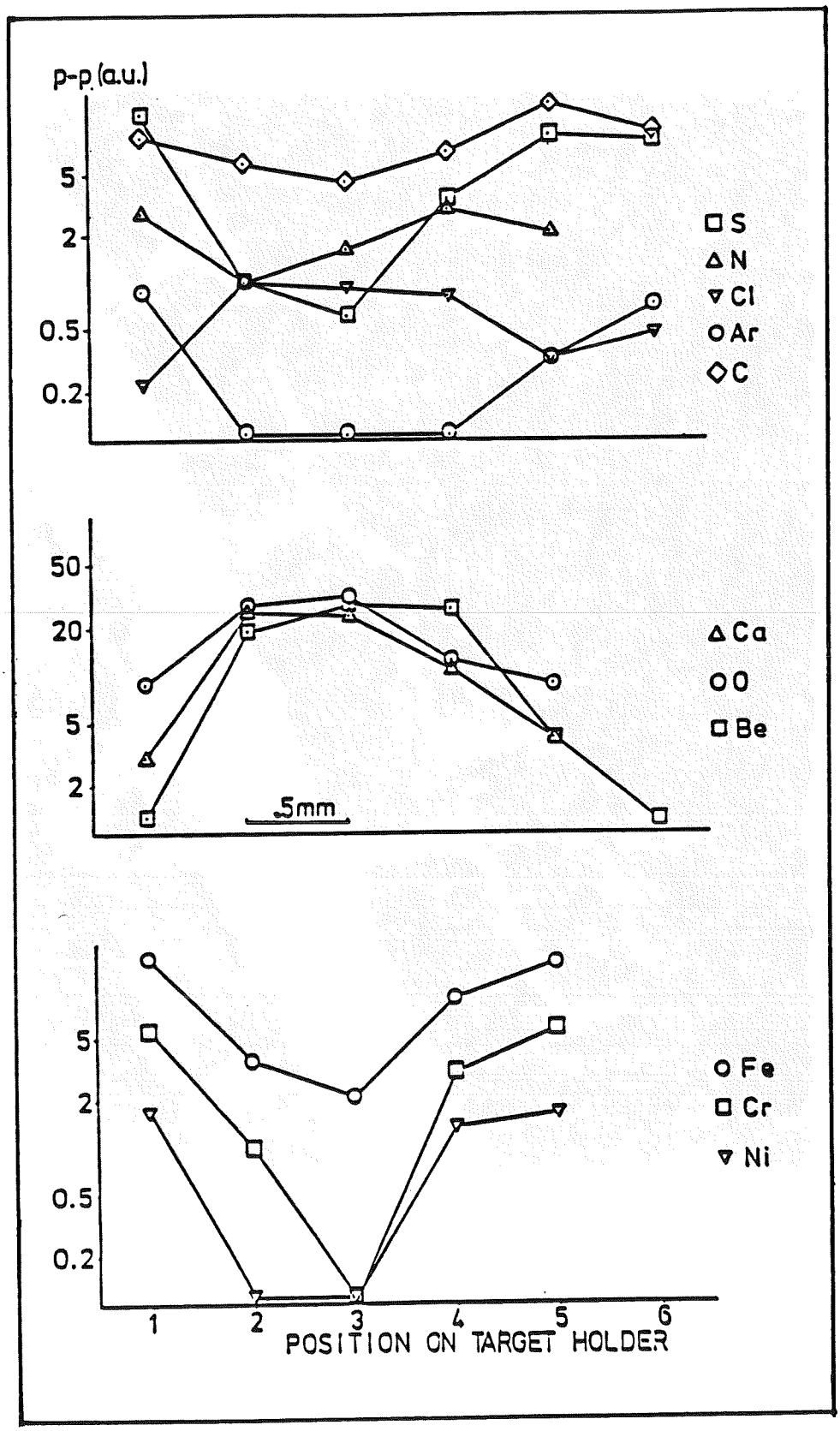

Fig. 9: Local variation of foreign atoms on the stainless-steel wall sample No. 6. The figure shows the spotwise deposition of BeO on the torus wall.

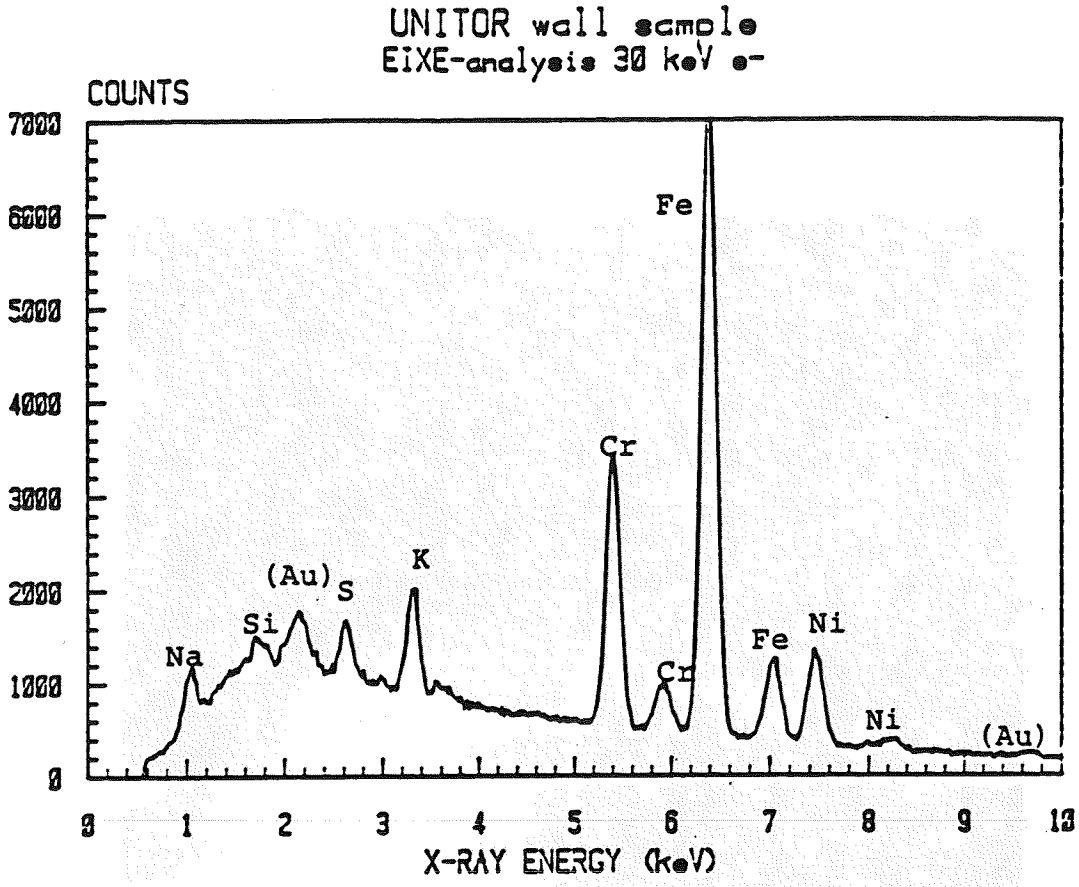

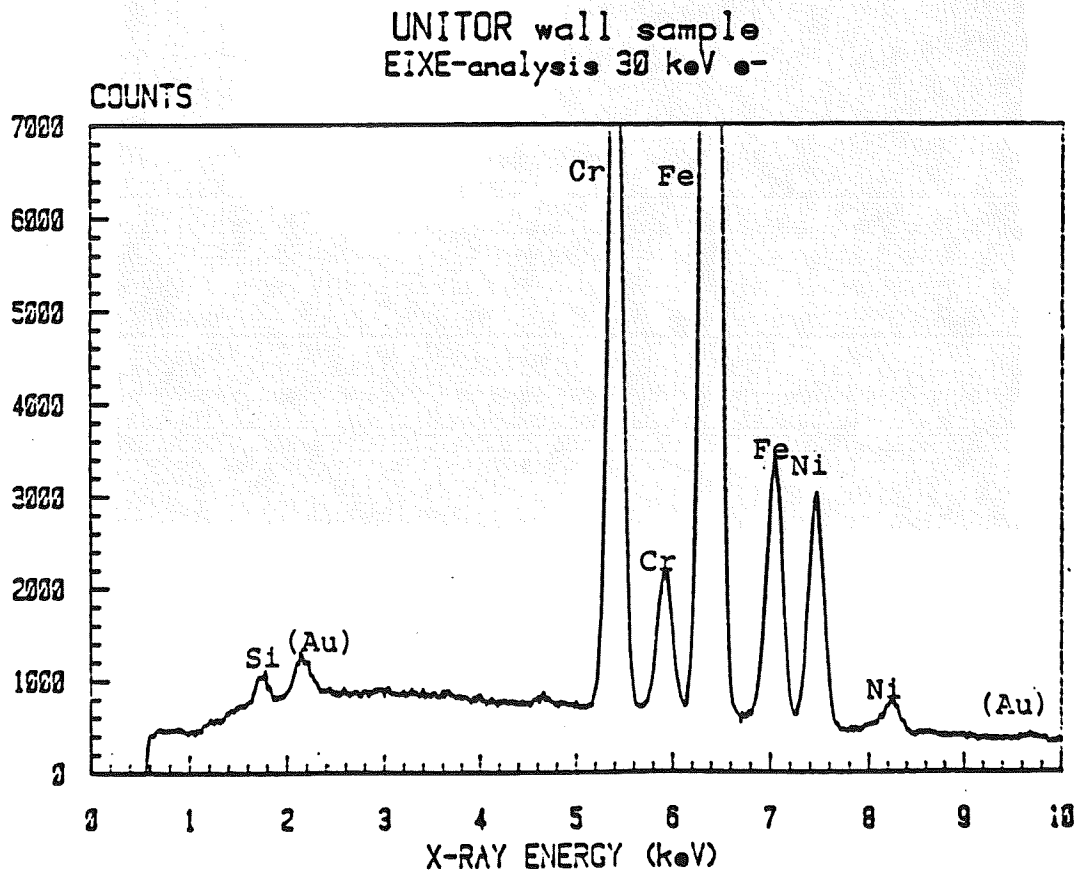

Fig. 10: EIXE spectrum of a beryllium droplet (identified by the characteristic co-elements Na, Si, S, K) on wall sample No. 6. For comparison, a spectrum of a point in the vicinity showing only stainless-steel components is plotted, too.

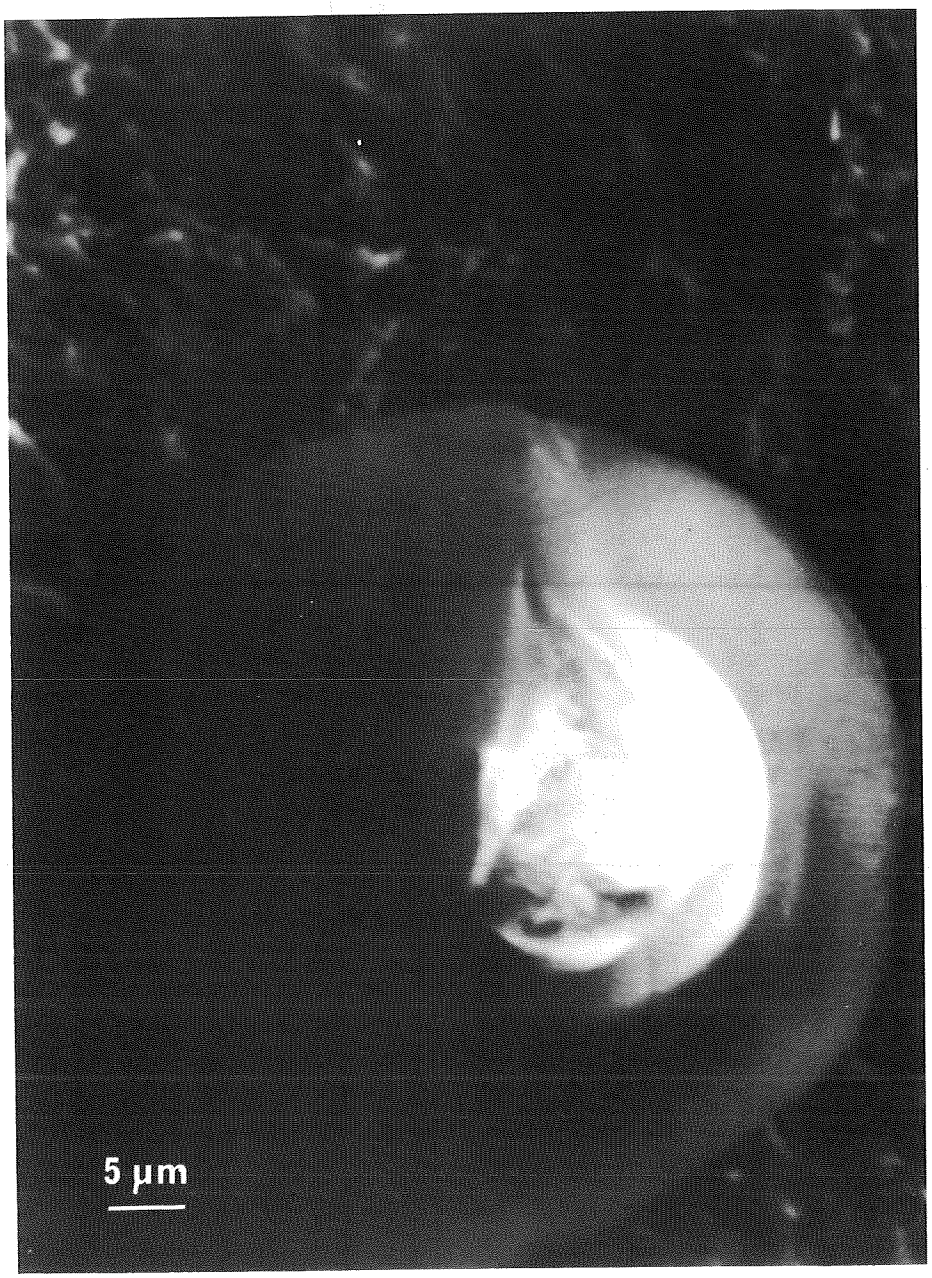

Fig. 11: A SEM picture of the area where the spectrum of fig. 10 was taken shows a spherical object with a diameter of about 50 µm.

Fig. 12: Stainless-steel splash on the wall sample. Many of these splashes and droplets are found on the samples.